

## The Electrostatic Field of B-DNA

Richard Lavery, Alberte Pullman, and Bernard Pullman

Institut de Biologie Physico-Chimique, Laboratoire de Biochimie Théorique associé au C.N.R.S.,  
13, rue Pierre et Marie Curie, F-75005 Paris, France

The electrostatic field associated with one complete turn of B-DNA is presented. Two base sequences poly (*dG*) · poly (*dC*) and poly (*dA*) · poly (*dT*) are studied and the effects of sodium counterions bound to the nucleic acid are investigated. The contrasts between the electrostatic potential and the electrostatic field of the macromolecules are discussed and the possible applications of the field are considered.

**Key words:** B-DNA—Electrostatic potential—Electrostatic field.

### 1. Introduction

In recent times the electrostatic potentials of molecules have been recognised as a most useful guide for obtaining information on their reactive and interactive properties [1–4]. This approach is particularly interesting for the study of macromolecules for which, with the aid of an appropriate technology, electrostatic potentials may be obtained at relatively low cost and yet give many insights into their chemical behaviour [3, 4].

Our laboratory has carried out an extensive study [3–7] of the electrostatic potentials of the nucleic acids, which has clarified many of their experimentally observed reactive properties, notably towards electrophilic attacking species. The association of these latter species, which often in their active form carry a positive charge, with the poly-anionic nucleic acids, constitutes a system ideally suited to study with the aid of electrostatic potentials, because the electrostatic term of their interaction energy is likely to be dominant, at least at long or intermediate interaction distances.

The scalar electrostatic potentials of the nucleic acids have indeed proven very helpful in describing what is “felt” by a charged species approaching the

macromolecule. In the present publication we shall introduce another aspect of the electrostatic properties of the nucleic acids, namely their vectorial electrostatic fields. These fields may be expected to provide information on the optimal approach path of a charged species towards the macromolecule, thus offering the possibility of obtaining a dynamic complement to the static studies made using potentials. Fields are, moreover, also adapted to describing what is "felt" by neutral dipolar molecules approaching the nucleic acid. By the term "dipolar" we imply those molecules for which a single center multipole expansion of the electron density would be dominated by the dipole term. In such cases, the electrostatic interaction energy of these species may be approximated by the scalar product of their dipole moments with the local field of the macromolecule. A particularly important species of this sort is water. Thus it is expected that a detailed knowledge of the field of macromolecules should provide a tool for investigating their zones of preferential hydration. In the present publication we present the methodology and the field generated by B-DNA and discuss briefly the results in this perspective.

## 2. Method

The calculation of the electrostatic field of macromolecules poses computational problems very similar to those encountered in calculating their electrostatic potentials. The field is, after all, very closely related to the potential, being simply its derivative with respect to distance. A most important distinction, however, introduced by this derivation is that the field is a vector quantity whereas the potential is only a scalar. The electrostatic field created at a point  $P$  by a molecule may be defined by:

$$E(P) = \sum \frac{Z_{\alpha} r_{\alpha P}}{|r_{\alpha P}|^3} - \int \frac{\rho(i) r_{iP}}{|r_{iP}|^3} d\tau_i$$

where the two terms represent, respectively, the nuclear field due to the nuclei of charge  $Z_{\alpha}$  distant by  $r_{\alpha P}$  and the electronic field due to the electron distribution  $\rho(i)$  whose volume element  $d\tau_i$  is at a distance  $r_{iP}$ .

Because of the close relationship between the potential and the field we have been able to retain, for the calculation of the field of DNA, two simplifications that we have previously developed in our studies of the potential. These simplifications are:

(1) The macromolecule is divided into a number of subunits. The electrostatic properties (potential or field) of the macromolecule are subsequently calculated by the superposition of the corresponding properties of the subunits, appropriately placed in space. In the case of the nucleic acids, the subunits, which are chosen to minimise the electronic perturbation caused by the subdivision, are phosphates, sugars and the nucleic acid bases, guanine, adenine, cytosine and thymine. The free valencies produced by the subdivision (the bonds involved being, the glycosidic bond, C3'-O3' and C5'-O5') are absorbed by adding hydrogen atoms [8].

(2) The electrostatic properties (potentials or fields) of the subunits are calculated with the aid of a multicentric multipole expansion of the electron density, the latter being obtained from an *ab initio* SCF wavefunction for the subunit, calculated with a standard basis set of gaussian orbitals contracted to minimal [9]. The multipole expansion employed, termed OMTP (overlap multipole expansion) [10], consists of a monopole, a dipole and a quadrupole centered on every atom of the subunit and at the mid-point of every atom pair. It is consequently a rather extensive expansion which has been shown to reproduce the exact electrostatic potential down to a distance of 2 Å from the constituent atoms of the subunit [11]. We have verified that this same expansion may also be employed to calculate accurate electrostatic fields down to the same approach limit.

The  $x$  components of the electrostatic field at a point  $P$  due to the monopole, dipole and quadrupole terms of the multipole expansion centered at a point  $S$  are respectively:

$$E_x^q(P) = \frac{qx}{|r_{SP}|^3}$$

for a monopole  $q$ ,

$$E_x^\mu(P) = \frac{1}{|r_{SP}|^3} \left( \frac{3x(r_{SP} \cdot \mu)}{|r_{SP}|^2} - \mu_x \right)$$

for a dipole  $\mu$ ,

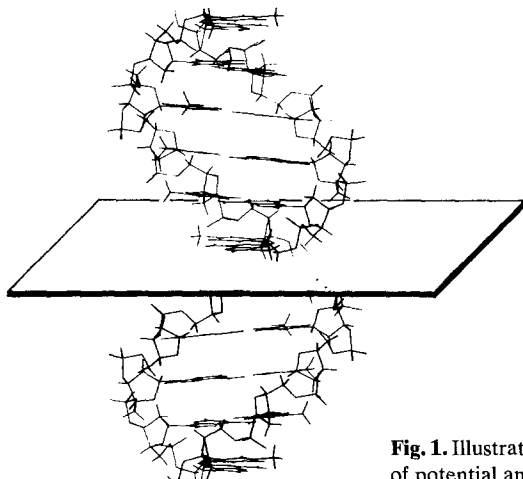
$$E_x^\theta(P) = \frac{3|\theta|(r_{SP} \cdot \theta)}{|r_{SP}|^5} - \frac{5x(r_{SP} \cdot \theta)}{2|r_{SP}|^2} - \frac{3x|\theta|}{2|r_{SP}|^5} - \frac{3|\theta|\theta_x(r_{SP} \cdot \theta)}{|r_{SP}|^5}$$

for an axial quadrupole  $\theta$ ,

where  $x$ ,  $\mu_x$  and  $\theta_x$  stand for the  $x$  components of  $r_{SP}$ ,  $\mu$  and  $\theta$ , respectively.

In the present publication we will study a model of B-DNA consisting of one turn of the double helix with 11 phosphates in each strand and the homopolymeric base sequences  $(GC)_n$  or  $(AT)_n$ . The geometry employed for the nucleic acid is that due to Arnott and Hukins [12].

The results of both potential and field calculations are presented in two different forms. Firstly, in planes cutting through the nucleic acid perpendicular to its helical axis, in the middle of the model double helix (see Fig. 1) and, secondly, on surface envelopes surrounding the macromolecule [13]. These surfaces, formed by the intersection of spheres centered on every atom of the macromolecule, with radii proportional to their van der Waals radii (a proportionality factor of 1.7 has been employed as in our preceding studies [4, 13]), enable an overall view of the potential or field around the nucleic acid and are particularly useful in revealing the electrostatic properties of the grooves formed by the double helical structure. In the case of the electrostatic fields, both the intensity and the direction of the field are given by appropriate graphic representations.



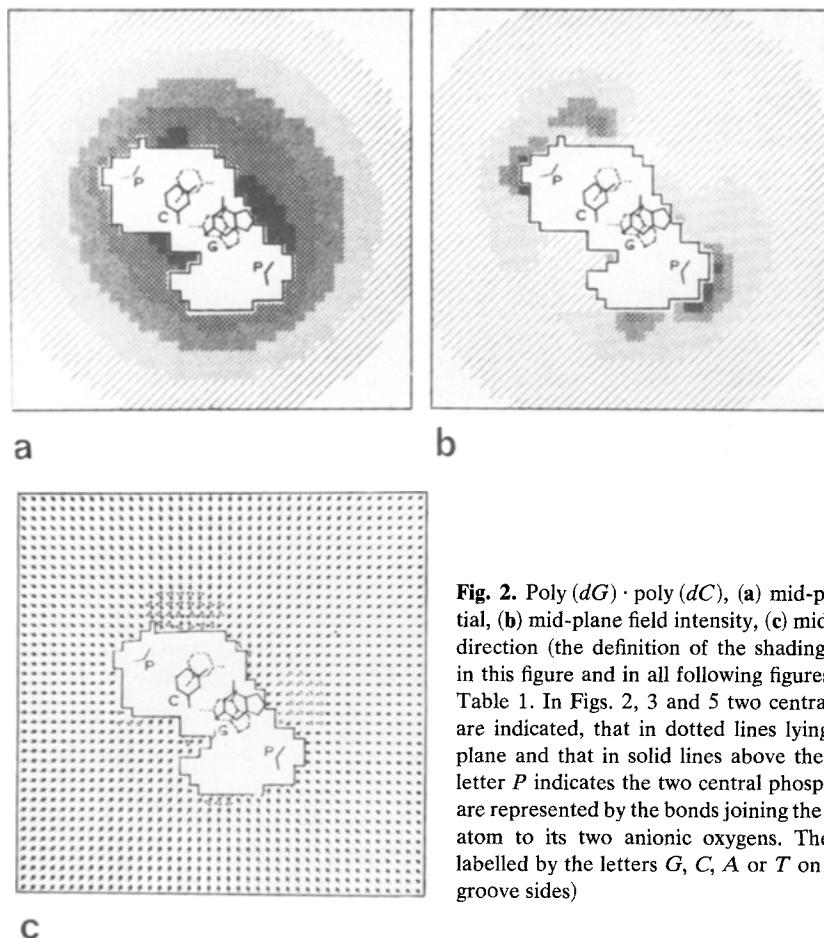
**Fig. 1.** Illustration of the mid-plane used for the calculations of potential and field

In our previous publications concerning electrostatic potentials the results have actually been presented in units of energy, namely kcal/mole, corresponding to the potential energy gained by a proton brought from infinity to the point under consideration. In the present publication we will use, in preference, more usual units of potential, namely volts, so as to allow easier comparisons with the electrostatic fields, which will be quoted in volt/Å. The conversion between kcal/mole and volt is made very simply by dividing the former by the factor 23.06.

### 3. Results and Discussion

The most important point that we wish to make in this study is the contrast in the appearance of B-DNA viewed in terms of electrostatic potential and viewed in terms of electrostatic field. Thus Fig. 2a presents the potentials due to the B-DNA model, with the base sequence  $(GC)_n$  in a plane perpendicular to its helical axis and passing through its center. The graduations in the potential are shown by various degrees of shading which are defined in Table 1. (Compare with isopotential curves of Ref. [14]). The central zone in the figure is a forbidden zone where the potentials of the macromolecule cannot be calculated with multipole expansions due to their associated approach limit. The distribution of potential is seen to be roughly circular, when distant from the nucleic acid, but upon approaching the macromolecule more closely the strongest potentials (the most darkly shaded zones) are seen to occur on the contours of the base pairs, that is, within the grooves of the double helix. The location of the potential minimum, indicated by the black dot in Fig. 2a, is found to be a function of the base sequence, occurring in the major groove for the sequence poly  $(dG) \cdot$  poly  $(dC)$ , presently considered and, as will be seen later, in the minor groove for the sequence poly  $(dA) \cdot$  poly  $(dT)$ .

This was one of the most significant findings of our studies of the electrostatic potential of DNA and it is of considerable importance in explaining the reactivity





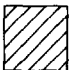

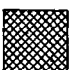


**Fig. 2.** Poly (*dG*) · poly (*dC*), (a) mid-plane potential, (b) mid-plane field intensity, (c) mid-plane field direction (the definition of the shadings employed in this figure and in all following figures is given in Table 1. In Figs. 2, 3 and 5 two central base pairs are indicated, that in dotted lines lying below the plane and that in solid lines above the plane. The letter *P* indicates the two central phosphates which are represented by the bonds joining the phosphorus atom to its two anionic oxygens. The bases are labelled by the letters *G*, *C*, *A* or *T* on their minor groove sides)

of the nucleic acid bases towards electrophiles. It has been found, moreover, that the dominance of the groove potentials is also a feature of other DNA conformations, such as *A*, *C*, and left-handed *Z*-DNA [3, 4].

We remark that the magnitudes of the potentials in Fig. 2a are very large, of the order of  $-10$  to  $-28$  volts (see Table 1). This is due to the combined effect of the 22 anionic phosphate groups in the model double helix, when they are, as in the calculations leading to Fig. 2a, unscreened by counterions.

In Fig. 2b the intensity of the electrostatic field in the same midplane is presented, shading once again being used to indicate the values, darker zones implying stronger fields (see Table 1 for details). At large distances from the macromolecule, the field intensity, like the potential, is roughly circular, but closer, a distribution quite unlike that of the potential is revealed. The strongest fields in Fig. 2b can be seen to be around the phosphate groups through which the mid-plane cuts, while the fields on the contours of the base pairs are relatively

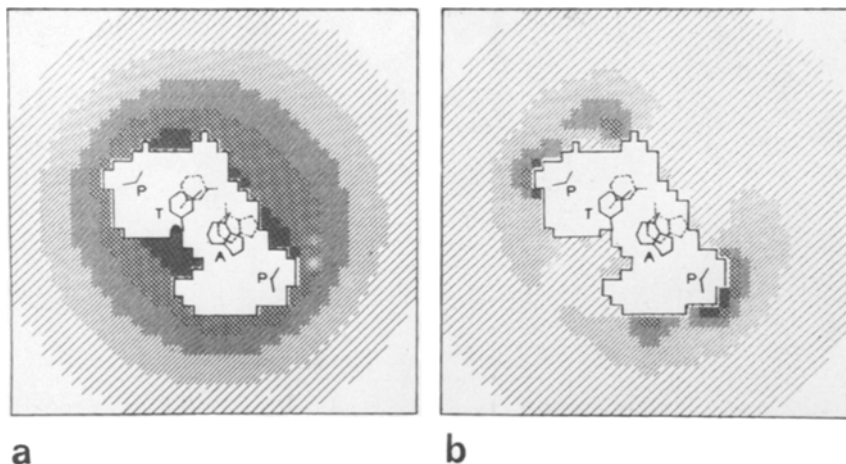
**Table 1.** Shadings used for the mid-plane and surface graphics (potentials in volt and fields in volt/Å)

Shading	Unscreened				Screened by Na <sup>+</sup>			
	Mid-Plane Potl.	Field	Surface Potl.	Field	Mid-Plane Potl.	Field	Surface Potl.	Field
	-10.40	0.0	-21.12	0.0	3.47	0.0	3.68	0.0
	↓	↓	↓	↓	↓	↓	↓	↓
	-13.27	0.47	-22.16	0.43	1.95	0.47	2.25	0.50
	↓	↓	↓	↓	↓	↓	↓	↓
	-16.17	0.93	-22.16	0.87	-0.44	0.93	0.80	1.00
	↓	↓	↓	↓	↓	↓	↓	↓
	-19.03	1.40	-24.28	1.30	-1.08	1.40	-0.65	1.50
	↓	↓	↓	↓	↓	↓	↓	↓
	-21.94	1.87	-25.36	1.73	-2.60	1.87	-2.08	2.00
	↓	↓	↓	↓	↓	↓	↓	↓
	-24.85	2.33	-26.45	2.17	-4.12	2.33	-3.51	2.50
	↓	↓	↓	↓	↓	↓	↓	↓
	-27.76	2.80	-27.53	2.60	-5.68	2.80	-4.98	3.00

weak. This is a very important change which we will discuss further, but first we present, in Fig. 2c, the directions associated with the field in the mid-plane.

These directions are indicated by three graphic symbols: an arrow if the local field vector is inclined by less than 30 degrees with respect to the plane, above or below; a triangle if the vector is inclined by more than 30 degrees above the plane; a distorted cross if the vector is inclined by more than 30 degrees below the plane. Each of these symbols is also oriented to show the direction of the component of the local field vector in the plane. In the case of the triangle and the distorted cross the vectorial direction indicated is from the wider end of the symbol towards its narrower end.

The results in Fig. 2c show that, overall, the field is radially directed towards the nucleic acid, the vectors lying more or less within the plane studied. This is clearly due to the large number of negative charges carried by the macromolecule, which, in this figure, shows field directions somewhat similar to those of a charged cylinder. In two zones, closer to the nucleic acid and on the side of the major groove, the field vectors leave the midplane to point towards two phosphates, which lie just below the plane for the strand towards the top of Fig. 2c and just above the plane for the other strand. It is because the anionic oxygens of the phosphates are turned towards the midplane on this side of the double helix that they are able to influence the field direction. Otherwise, there is little fine

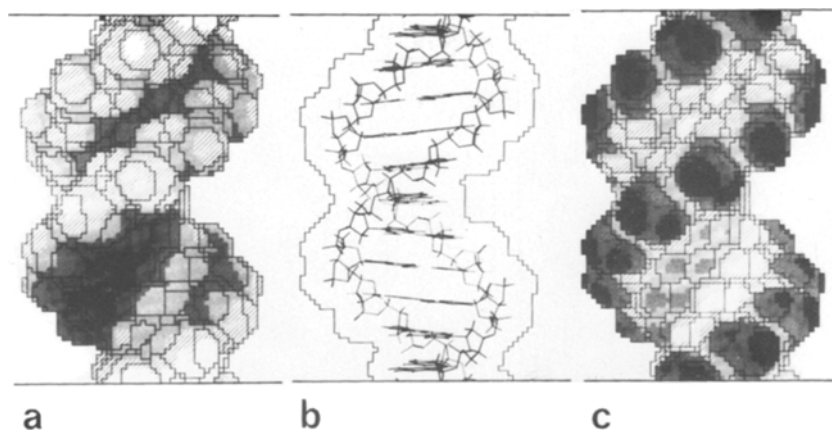


**Fig. 3.** Poly (*dA*) · poly (*dT*), (a) mid-plane potential, (b) mid-plane field intensity

structure in this diagram for the unscreened nucleic acid, but, as we will show later, this is no longer the case when screening counterions are present.

The results for poly (*dA*) · poly (*dT*) are very similar in their general aspect to those for poly (*dG*) · poly (*dC*), although they differ by certain details. From Fig. 3a, it is confirmed that the strongest potentials are again associated with the contours of the base pairs but that, as we have mentioned, the position of the potential minima has moved into the minor groove for this base sequence. The field distribution, shown in Fig. 3b, is similarly affected by the base sequence, the fields being somewhat weaker on the major groove side and somewhat stronger on the minor groove side (as were the potentials). The magnitude of the maximal field, on the phosphate backbone, is, however, almost identical for the two sequences (the values being 2.63 volt/Å for poly (*dG*) · poly (*dC*) and 2.61 volt/Å for poly (*dA*) · poly (*dT*)). The field directions for poly (*dA*) · poly (*dT*) are not shown as they are almost indistinguishable from those given in Fig. 2(c).

Let us now consider the potential and field distributions on the surface envelopes surrounding the nucleic acid. In Fig. 4, which represents calculations for the poly (*dG*) · poly (*dC*) model, the central diagram 4b recalls the molecular structure of the model, the left hand diagram 4a shows the potential distribution on the corresponding surface and the right hand diagram 4c, the field distribution (for details of the shadings employed refer to Table 1). This graphic representation renders the grooves of the double helix easily visible, the minor groove appearing in the upper half of these diagrams and the major groove in the lower half. The distinction between potentials and fields is again very clear. The strongest potentials are in the grooves and the strongest fields are on the anionic oxygens of the phosphates. The dominance of the major groove over the minor groove in terms of potentials or fields for the (*GC*)<sub>*n*</sub> sequence is also confirmed from this figure.



**Fig. 4.** Poly(*dG*) · poly(*dC*), (a) potential on the molecular surface envelope, (b) diagrammatic representation of a helix turn, (c) field on the molecular surface envelope

For the sake of space we do not reproduce here the graphical representations of the corresponding results for the (*AT*)<sub>*n*</sub> sequence of B-DNA. However, we present, in Table 2, a quantitative comparison of the two grooves and of the phosphodiester strands for the two sequences. The strongest potentials and the strongest fields found on the surface of certain selected atoms in the surface envelopes are given and the values in this table confirm what has been shown graphically for the unscreened double helices. We will return to the remaining entries shortly.

Why are the distributions of the potential and of the field so different? The answer lies in the dependence on the distance (from the charge distribution) of the potential or the field at a given point in space. The field, being the derivative of the potential, has a higher inverse power dependence on the distance. In practical terms this means that the parts of the charge distribution which are more distant from the point at which the values are calculated play a less important role in determining the field than in determining the potential. For our model nucleic acid the result is striking. The long range of the potentials of its constituent subunits leads to important superposition effects. Notably, they sum to yield potentials higher in the grooves of the double helix than close to any of the phosphates, although these groups, when isolated, are associated with the strongest potentials. The shorter range of the electrostatic field attenuates these superposition effects and the strongest fields are found close to the charged phosphates which, when isolated, are also associated with the strongest fields (a maximum of 2.54 volt/Å being calculated for the phosphate, at the approach limit of 2 Å, compared to approximately 1.5 volt/Å for the nucleic acid bases). Let us now investigate the effect of the presence of counterions on the electrostatic properties of B-DNA. This is an important extension as such ions are known to be closely associated with the nucleic acid in solution. In this paper we present the results for only one simple, saturated screening of the phosphates, that we have employed in our previous publications [4, 15] and which consists of binding

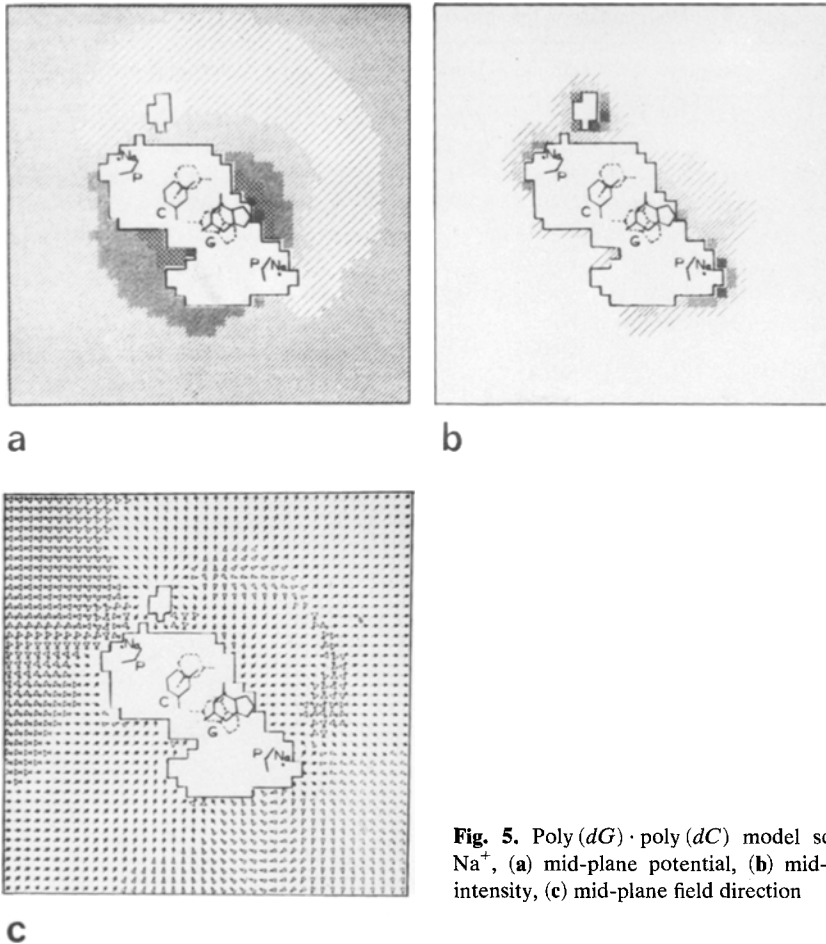


**Table 2.** Punctual fields and potentials on the surface of B-DNA

Property	Region	Atom	Unscreened		Screened by Na <sup>+</sup>	
			(GC) <sub>n</sub>	(AT) <sub>n</sub>	(GC) <sub>n</sub>	(AT) <sub>n</sub>
Field (volt/Å)	Minor groove	N3(G)	1.32		1.13	
		O2(C)	1.20		1.01	
		N3(A)		1.32		1.17
		O2(T)		1.24		1.07
	Major groove	N7(G)	1.51		1.44	
		O6(G)	1.39		1.35	
		N7(A)		1.26		1.15
		O4(T)		1.06		1.02
	Backbone phosphate anionic oxygens		2.59	2.58	2.92	2.85 (on Na <sup>+</sup> )
	Minor groove	N3(G)	-26.32		-4.21	
		O2(C)	-26.23		-4.08	
		N3(A)		-27.14		-4.99
O2(T)			-27.27		-5.03	
Potential (volt)	Major groove	N7(G)	-27.49		-4.73	
		O6(G)	-27.36		-4.64	
		N7(A)		-25.97		-2.86
		O4(T)		-25.36		-2.73
	Backbone phosphate anionic oxygens		-26.62	-26.02	-2.95	-2.34 (on Na <sup>+</sup> )

a sodium cation in a bridged position between the two anionic oxygens of each phosphate group, 2.15 Å from each oxygen and in the plane containing these atoms and the phosphorus atom. This is not intended to be a realistic distribution of counterions, particularly for sodium, as the evidence would suggest that these ions, in contrast to magnesium ions, are not site-bound to the nucleic acid [16, 17]. Our previous studies have shown, however, at least for the *B* conformation of DNA, that the exact nature of the saturated counterion distribution, or the type of cation employed, have relatively little effect on the resulting, qualitative electrostatic properties of the screened acid [18, 19].

Returning to the mid-plane representation, Fig. 5a shows the potentials for our screened poly(*dG*) · poly(*dC*) model. As described in our earlier work [4, 18, 19], the effect of screening B-DNA is principally to reduce the absolute magnitudes of the potentials, without greatly changing their distribution. The strongest potentials are seen to be associated with the contours of the base pairs, the minimum potential, moreover, being still on the major groove side of *GC*, as in the unscreened double helix (for details of shading see Table 1). At



**Fig. 5.** Poly(*dG*) · poly(*dC*) model screened by  $\text{Na}^+$ , (a) mid-plane potential, (b) mid-plane field intensity, (c) mid-plane field direction

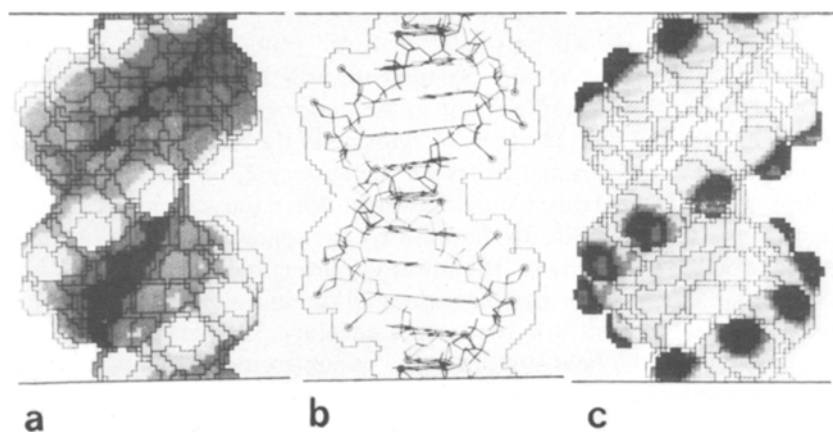
intermediate distances there is, however, a slight imbalance caused by the counterions, which makes the potentials in the major groove somewhat less negative than those on the opposing side. This is due to the orientation of the phosphate groups in B-DNA which is such that their anionic oxygens are turned more towards the major groove. This in turn places the screening counterions closer together on this side of the double helix and hence, by increased superposition of potentials, increases their local screening effect.

How the electrostatic fields have been affected by the counterions may be seen from Figs. 5b and 5c. Fig. 5b shows that the strongest fields are highly concentrated around the screening cations themselves. This is particularly clear when comparing Figs. 2b and 5b (for which the definitions of the shading are identical). Such a result may be understood because the zwitterionic pair formed by the phosphate-sodium ion interaction is a zone where the gradient of the potential will be very large. The maximum field intensity for the screened model,  $2.70 \text{ volt}/\text{\AA}$  is also, not surprisingly, stronger than that of the unscreened acid,  $2.63 \text{ volt}/\text{\AA}$ , but the strong fields occur only very close to the ion pairs.

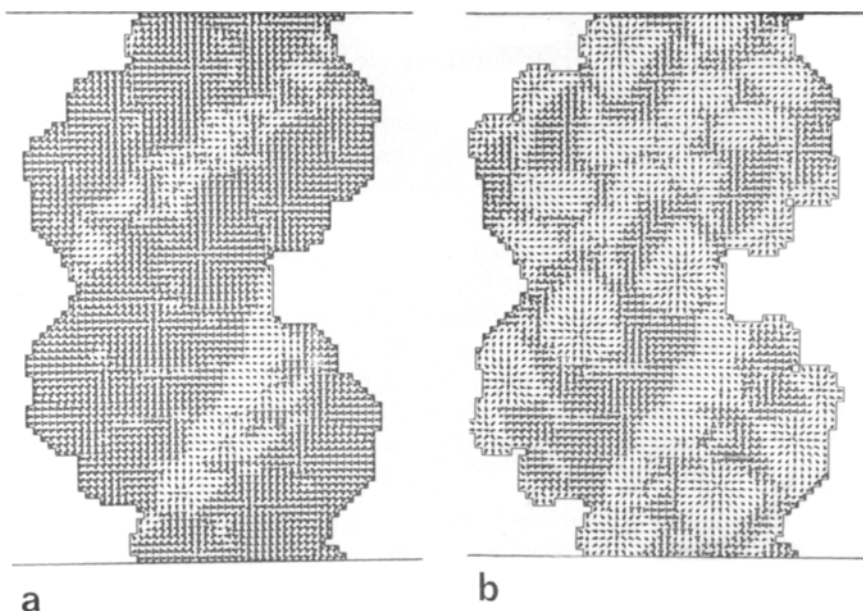
The field direction (Fig. 5c), is very considerably changed by the counterions. Whereas, before screening, the field was oriented radially towards the nucleic acid (see Fig. 2c), this orientation prevails now only on the side of the minor groove. From the helical strands the field points outwards (and up or down due to the displacement out of the plane of the closest sodium ions) and this is also the direction of the field on the major groove side at long distance. Closer to the nucleic acid there is an apparent “bridge” formed by field lines which spreads across the entrance to the major groove. This is caused by successively bound sodium ions below the plane for the upper half of the “bridge” and above the plane for the lower half. The effect of these more distant counterions is visible on this side of the double helix because of the orientation of the phosphates which causes these ions to be considerably closer to the mid-plane than the phosphate groups to which they are bound. This field vector “bridge” may be correlated with the barrier of weaker potential on the major groove side of the double helix, visible in Fig. 5a.

We have also calculated the potentials and fields on the surfaces of the screened B-DNA models. The results for poly(*dG*) · poly(*dC*) are compared in Fig. 6 where, once again, the central diagram 6b represents the molecular structure, the left hand diagram 6a shows the distribution of the potential and the right hand diagram 6c, the distribution of the field (for details of the shading used see Table 1). As in the mid-plane, the distinction between the potential and the field is clear. The most negative potentials in the screened model lie in the grooves and, for this sequence (*GC*)<sub>*n*</sub>, the minimum is within the major groove. The field distribution, in contrast, shows the strongest fields rightly concentrated around the screened phosphates and particularly on the surface of the screening counterions themselves.

The directions associated with the electrostatic fields on the surface of our poly(*dG*) · poly(*dC*) model are given in Figs. 7a and 7b. The first of these



**Fig. 6.** Poly(*dG*) · poly(*dC*) model screened by Na<sup>+</sup>, (a) potential on the molecular surface envelope, (b) diagrammatic representation of a helix turn, (c) field on the molecular surface envelope



**Fig. 7.** Poly (*dG*) · poly (*dC*), (a) field direction on the molecular surface envelope without screening Na<sup>+</sup> ions, (b) field direction on the molecular surface envelope with screening Na<sup>+</sup> ions

figures contains the field directions for the unscreened model and the second for the screened model. A graphic technique similar to that used for the field direction in the mid-plane has been employed. The three graphic symbols are the same, but now they indicate the direction of the local field vector with respect to a plane locally tangential to the spherical surface of the atom forming part of the surface envelope. Field vectors within 30 degrees of this plane are thus shown by the arrow, vectors pointing outwards from the surface by more than 30 degrees are indicated by the triangle and vectors pointing inwards by more than 30 degrees are shown by the distorted cross

The results for the unscreened poly (*dG*) · poly (*dC*) model in Fig. 7a show, principally, circular zones of vectors pointing towards the phosphate anionic oxygens, the N7 and O6 atoms of guanine in the major groove and towards the N3 atoms of guanine and the O2 atoms of cytosine in the minor groove. In the major groove there are also small zones on the surface covering the cytosine amino groups where the field direction is outwards. When the screening counterions are added, the results in Fig. 7b show clearly the concentrations of outward pointing field around these cations. The inward pointing field zones around the phosphate anionic oxygens are now considerably diminished and the fields in the groove are largely aligned with the surface envelope. One may also note an interesting tendency of the field vectors in the minor groove to point from the purine strand towards the pyrimidine strand.

In order to limit the size of the publication, the results for screened poly (*dA*) · poly (*dT*) are not shown, but Table 2 contains punctual values of the

greatest potentials and fields on the surfaces of selected atoms for the two base sequences studied. These results enable us to see how screening has opposing effects on potential and field in three ways:

Firstly, as already seen, screening strongly decreases the magnitude of the potentials all around the nucleic acid. The effect on the fields is less uniform and although the fields in certain areas are decreased, the fields close to the screened phosphates are increased.

Secondly, screening increases the difference in potential between the grooves and the backbones of the double helix, in favour of the bases. Screening also increases the difference in the field, but now this increase is in favor of the backbones.

Finally, screening decreases the distinction between the potential in the two grooves of the  $(GC)_n$  sequence and increases the distinction for the  $(AT)_n$  sequence. This is again due to the relatively greater concentration of the counterions on the side of the major groove of the double helix, where, consequently, their attenuating effect on the negative potentials is greater. Hence for  $(GC)_n$ , where the major groove is favoured when unscreened, screening diminishes the difference and for  $(AT)_n$ , where the minor groove was already favoured, screening enhances the difference. In terms of field, as the counterions increase the magnitude of the field in their neighbourhood we expect a reversal of the phenomena observed for the distribution of the potential and this is indeed the case: screening increases the distinction between the fields in the grooves of  $(GC)_n$  and decreases it for  $(AT)_n$ .

#### 4. Conclusions and Perspectives

The study of the electrostatic field of B-DNA that we have presented shows many interesting features which may have important chemical or biochemical implications. In a forthcoming publication we will show the precision with which this field may be used to describe the binding sites and energies of small, neutral, dipolar molecules. Such an application is of particular interest in the case of water molecules hydrating the nucleic acid. Anticipating this detailed analysis, we can already make some qualitative predictions based on the most clearly defined features of the field distributions:

- (1) Water molecules should bind most strongly to the phosphate groups of the nucleic acid.
- (2) Those water molecules which do bind in the grooves should exhibit preferences for the major or minor groove depending on the base sequence. The most important distinction being for the  $(GC)_n$  sequence where the major groove is considerably more favoured than the minor groove.
- (3) For the preferred binding mode of the water molecules, the field direction may be a useful guide, the water dipole having a natural tendency to align with this direction.

(4) The presence of screening cations bound to the nucleic acid phosphates should increase the binding energy of water in these regions and, concurrently, decrease the binding energy of water in the grooves of the double helix.

The second possible use of the electrostatic field is as a guide to the approach path of charged reactive species towards the nucleic acid. This aspect of our present findings will also be exploited in forthcoming studies where we shall attempt to model dynamically the interaction between biologically important electrophiles and DNA.

A final remark that we wish to make concerns the contrasts between the appearance of B-DNA viewed in terms of electrostatic potential and viewed in terms of electrostatic field. This implies that when a reaction of DNA with a charged reactive species takes place in aqueous solution, the reactant and the solvent will be under very different influences from the macromolecule, insofar as the former will be dominated by the potential and the latter by the field. This is an important feature to bear in mind if the possibilities of competition between these two species for a given site on DNA are to be understood.

*Acknowledgment.* This work was supported by the National Foundation for Cancer Research (U.S.A.) to which the authors wish to express their thanks.

## References

1. Scrocco, E., Tomasi, J.: *Top. Curr. Chem.* **42**, 95 (1973)
2. Scrocco, E., Tomasi, J.: *Int. J. Quant. Chem.* **11**, 115 (1978)
3. Pullman, A., Pullman, B.: in *Chemical applications of atomic and molecular electrostatic potentials*, ed. Politzer, P., Truhlar, D. G., p. 381, New York: Plenum (1981)
4. Pullman, A., Pullman, B.: *Quart. Rev. Biophysics* **14**, 289 (1981)
5. Pullman, B., Perahia, D., Cauchy, D.: *Nucl. Acids Res.* **6**, 3821 (1979)
6. Zakrzewska, K., Lavery, R., Pullman, B.: in *Biomolecular stereodynamics*, ed. R. H. Sarma, p. 163, Adenine Press (1982)
7. Pullman, B., Lavery, R., Pullman, A.: *Eur. J. Biochem.*, **124**, 229 (1982)
8. Pullman, B.: in *New horizon in biological chemistry*, p. 31, Tokyo: Japan Scientific Societies Press (1981)
9. Pullman, B., Gresh, N., Berthod, H., Pullman, A.: *Theoret. Chim. Acta (Berl.)* **44**, 151 (1977)
10. Port, G. N. J., Pullman, A.: *FEBS Lett.* **31**, 70 (1973)
11. Goldblum, A., Perahia, D., Pullman, A.: *Int. J. Quant. Chem.* **15**, 121 (1979)
12. Arnott, S., Hukins, D. W. L.: *Biochem. Biophys. Res. Commun.* **47**, 1504 (1972).
13. Lavery, R., Pullman, B.: *Int. J. Quant. Chem.* **20**, 259 (1981)
14. Perahia, D., Pullman, A., Pullman, B.: *Int. J. Quant. Chem. Quant. Biol. Symp.* **6**, 353 (1979)
15. Perahia, D., Pullman, A., Pullman, B.: *Theoret. Chim. Acta (Berl.)* **51**, 349 (1979)
16. Manning, G. S.: *Quart. Rev. Biophys.* **11**, 179 (1978)
17. Bleam, M. L., Anderson, C. F., Record Jr., M. T.: *Proc. Natl. Acad. Sci. USA* **77**, 3085 (1980)
18. Lavery, R., Cauchy, D., Rojas, O., Pullman, A.: *Int. J. Quant. Chem., Quant. Biol. Symp.* **7**, 323 (1980)
19. Cauchy, D., Lavery, R., Pullman, B.: *Theoret. Chim. Acta (Berl.)* **57**, 323 (1980)

Received April 15, 1982